Title

18-year land-surface hydrology model simulations for a midlatitude grassland catchment in Valdai, Russia

Journal

Monthly Weather Review, 125(12)

ISSN

0027-0644

Authors

Schlosser, CA
Robock, A
Vinnikov, KY
et al.

Publication Date

1997

DOI

10.1175/1520-0493(1997)125<3279:YLSHMS>2.0.CO;2

Peer reviewed

18-Year Land-Surface Hydrology Model Simulations for a Midlatitude Grassland Catchment in Valdai, Russia

C. ADAM SCHLOSSER

Geophysical Fluid Dynamics Laboratory/NOAA, Princeton, New Jersey

ALAN ROBOCK AND KONSTANTIN YA. VINNIKOV

Department of Meteorology, University of Maryland at College Park, College Park, Maryland

NINA A. SPERANSKAYA

State Hydrological Institute, St. Petersburg, Russia

YONGKANG XUE

Department of Geography, University of Maryland at College Park, College Park, Maryland

(Manuscript received 23 May 1996, in final form 24 April 1997)

ABSTRACT

Off-line simulations of improved bucket hydrology and Simplified Simple Biosphere (SSiB) models are performed for a grassland vegetation catchment region, located at the Valdai water-balance research station in Russia, forced by observed meteorological and simulated actinometric data for 1966–83. Evaluation of the model simulations is performed using observations of total soil moisture in the top 1 m, runoff, evaporation, snow depth, and water-table depth made within the catchment. The Valdai study demonstrates that using only routine meteorological measurements, long-term simulations of land-surface schemes suitable for model evaluation can be made. The Valdai dataset is available for use in the evaluation of other land-surface schemes.

Both the SSiB and the bucket models reproduce the observed hydrology averaged over the simulation period (1967–83) and its interannual variability reasonably well. However, the models' soil moisture interannual variability is too low during the fall and winter when compared to observations. In addition, some discrepancies in the models' seasonal behavior with respect to observations are seen. The models are able to reproduce extreme hydrological events to some degree, but some inconsistencies in the model mechanisms are seen. The bucket model's soil-moisture variability is limited by its inability to rise above its prescribed field capacity for the case where the observed water table rises into the top 1-m layer of soil, which can lead to erroneous simulations of evaporation and runoff. SSiB's snow depth simulations are generally too low due to high evaporation from the snow surface. SSiB typically produces drainage out of its bottom layer during the summer, which appears inconsistent to the runoff observations of the catchment.

1. Introduction

Within the past decade, the range of complexity among the land-surface parameterizations used in general circulation models (GCMs) has grown significantly. Current land-surface models are based on a wide range of theoretical frameworks, ranging from a simple ''bucket'' hydrology (Budyko 1956; Manabe 1969), to a more sophisticated biosphere or ''big-leaf'' scheme [e.g., the Simple Biosphere (SiB) model (Sellers et al. 1986) and the Biosphere–Atmosphere Transfer Scheme (BATS) model (Dickinson et al. (1986)]. Recent studies have shown significant sensitivities to the choice of land-surface parameterizations for GCM applications (e.g., Rind et al. 1992; McKenney and Rosenburg 1993). However, these studies had no observations for model comparison and evaluation.

In an effort to improve our understanding and parameterizations of land-surface processes, a wide variety of observational and diagnostic modeling studies have been conducted. One widely used methodology involves ''off-line'' simulations of the land-surface schemes. The land-surface schemes are decoupled from the GCMs and forced by observational and/or simulated data (when needed). The prognostic outputs of the models are then compared to observed values.

Corresponding author address: Dr. C. Adam Schlosser, GFDL/NOAA, Princeton University, Forrestal Campus, U.S. Route 1, P.O. Box 308, Princeton, NJ 08542.
E-mail: cas@gfdl.gov

Calibration and verification studies using Amazon data (e.g., Sellers and Dorman 1987; Sellers et al. 1989; and Xue et al. 1996b) have addressed the parameterizations of land-surface processes for a tropical climate, but verification studies must also be performed for mid and high-latitude environments. Off-line studies of the Project for the Intercomparison of Land-Surface Parameterization Schemes (PILPS) (Henderson-Sellers et al. 1993) have recently used data from the Cabauw site in the Netherlands (Chen et al. 1996). The Cabauw data contained estimates of observed latent and sensible heat fluxes for model evaluation. However, the forcing data spanned only one year and the resulting spinup issues complicated the model analysis. In addition, an analysis of the interannual variability of the models could not be performed.

Robock et al. (1995; hereafter referred to as RO) used routine meteorological and actinometric data from six stations within midlatitude Russia spanning the years 1978–83 to perform off-line runs with a standard GCM bucket model (Manabe 1969) and the Simplified Simple Biosphere (SSiB) (Xue et al. 1991) model. The results revealed some discrepancies in both of the models, and subsequently, improvements to SSiB's runoff parameterization have been made (Xue et al. 1996a). However, the study lacked any model comparisons to observations of evaporation, runoff, and water-table depth, and the six years of forcing for the model simulations, the longest for off-line simulations to date, were still insufficient for an extensive interannual analysis. Further studies using different stations with more extensive data spanning longer time periods were strongly recommended by RO.

Recently, Vinnikov et al. (1996) described a unique set of data obtained from the Valdai water-balance research site in Russia. An extensive set of meteorological, hydrological, and actinometric measurements was gathered at three catchments within the research site for the years 1960 to 1990. The three catchments, Tayozhniy, Sinaya Gnilka, and Usadievskiy, each contained different dominant vegetation types: a mature forest, a growing forest, and grassland, respectively. Vinnikov et al. (1996) used routine soil moisture measurements taken within each catchment to perform an extensive statistical analysis of the characteristic temporal and spatial scales of soil moisture.

Our principal aim of this study is to demonstrate that an effective seasonal and interannual diagnostic analysis of off-line land-surface hydrology simulations—never before conducted—can be obtained using the Valdai data. We use meteorological data taken near the Usadievskiy (grassland) catchment and simulated radiation data to perform off-line simulations for a slightly modified bucket hydrology model (similar to that of the RO study) and the SSiB model. Overall, the Valdai simulations for the bucket and SSiB models demonstrate that various land-surface schemes are able to be forced with only routine meteorological data over many years to produce useful simulations for model evaluation. With the need for only meteorological data to force the models, the potential exists to utilize many datasets such as Valdai for off-line testing. The meteorological forcing dataset at Valdai spans 18 years (1966–83), allowing for much longer model simulations than previous studies. The Valdai dataset contains measurements of soil moisture, water table depth, runoff, snowcover, and precipitation within the catchment. Thus, the observed water balance for the catchment can be closed by calculating evaporation as a residual. In addition, a subset of evaporation estimates calculated by Fedorov (1977) is also used as further validation. The models are allotted a spinup period of 1 year determined from previous sensitivity tests (Schlosser 1995). The remaining portion of the simulation period, 17 years, is then used to verify against observations. The models' interannual and seasonal variability is evaluated, and the models' ability to reproduce extreme hydrologic events (e.g., droughts) is assessed.

In the next section, we describe the data of the Usadievskiy catchment at Valdai used for the simulation experiments. In section 3, we describe some improvements made to the parameters and codes of each of the models for the simulations, and outline the basic framework of the SSiB and bucket hydrologies. The results of the model simulations and a verification and intercomparison analysis are presented in section 4. Finally, discussions, conclusions, and closing remarks are given.

2. Data

The Valdai research station is located in a forest region south of St. Petersburg at 57.6°N, 33.1°E and contains an extensive set of water-balance observation catchments of different dominant vegetation type (Fedorov 1977 and Vinnikov et al. 1996). A summary of the current data collection is given in Table 1. The entire observational dataset obtained from Valdai spans the years 1960–90. This study focuses on the model simulations of the grassland catchment. The grassland catchment, Usadievskiy, is approximately 0.36 km^2.

a. Hydrological data

Within the Usadievskiy catchment, 11 representative sites (out of more than 100) were chosen for total soil moisture observations. Near the end of each month, a representative sample of soil cores is taken at each site, and the total soil moisture is measured by the thermostat-weight (gravimetric) technique (described in RO). The accuracy of the soil moisture measurements in the top 1-m layer is ± 1 cm (RO). The seasonal variations of total soil moisture in the top 1 m at each of the 11 measurement sites are very similar and their differences are mostly biases (Fig. 4 of Vinnikov et al. 1996). Therefore, we use the average value of the 11 measurement

TABLE 1. Valdai data collection.

Hydrological measurements for three different catchments—taken every month
Total soil moisture in the top 100 cm for 9–11 sites within each catchment, 1963–85
Catchment averaged total soil moisture in the top 20, 50, and 100 cm, 1960–90
Runoff, 1960–90
Depth of groundwater table, 1960–90
Water equivalent snow depth,* 1960–90
Precipitation, 1960–90
Radiative flux measurements—10 day averages of 3-h totals taken during growing season
Total solar radiation, 1960–90
Net shortwave radiation for
Various agricultural fields, 1967–88
Top of boreal forest, 1960–90
Boreal forest under the tree canopy, 1967–90
Albedo for
Natural meadow field, 1967–87
Top of boreal forest, 1960–90
Meteorological data (including precipitation) taken every 3 h, 1966–83

* Measurements of snow depth also taken after snow events and frequently during snowmelt.

FIG. 1. Map of the Usadievskiy catchment at Valdai. Water-table measurement sites are indicated by filled circles. Soil moisture measurement sites are indicated by filled squares. Open circles with dashed lines indicate the snow measurement sites and routes, respectively. Runoff is measured at the stream outflow point of the catchment located in the lower left-hand corner of the map and indicated by a bold bracket. The short dash line denotes the catchment boundary. Hatched areas denote regions of swampy conditions. Elevation contours are in increments of 2 m.

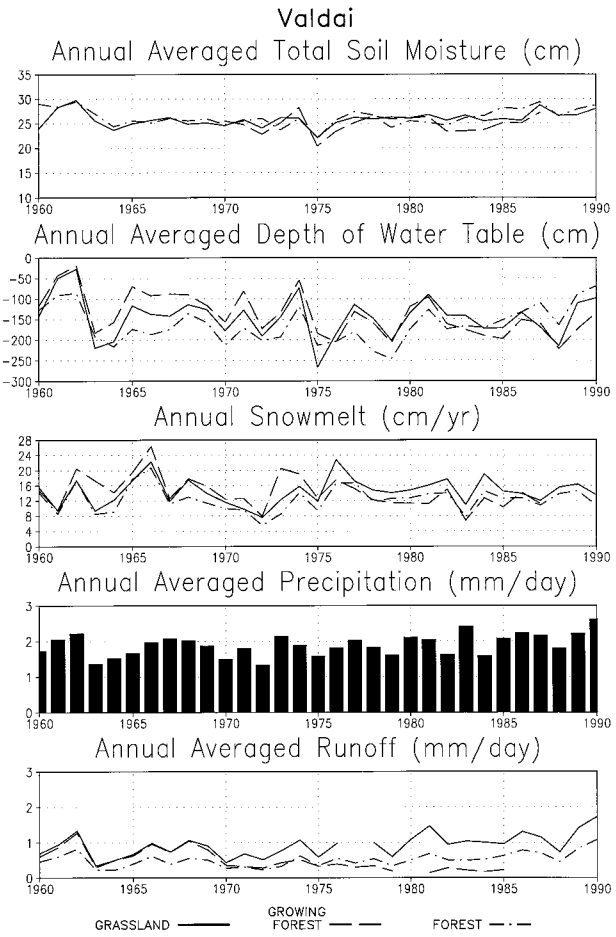

FIG. 2. Annual averaged values of observed total soil moisture, depth of water table, snowmelt, and runoff for the three catchments at Valdai. In addition, annual averaged observed precipitation measured near the grassland catchment is given.

sites for total soil moisture in the top 1 m to compare with the model simulations.

Runoff measurements are obtained by streamflow observations made at the outflow point of the catchment region (as indicated by a bracket in Fig. 1). Triangle weirs are used to measure the water level and are then translated into a water flux outflow from the catchment. A quantitative error analysis of the runoff measurements was difficult to obtain. Generally speaking, a high degree of confidence can be placed on the measurements made during the warmer months. During the colder months when the stream is typically frozen and the springtime when the stream typically overflows, the runoff measurements tend to be less accurate.

Numerous wells that measure water-table depth are located at various points within the catchment (Fig. 1). The water-table depth measurements obtained for this study are an average of all the measurements taken at each of the well sites within the catchment.

An example of the data available from the Valdai research site is given in Fig. 2. A similar figure was

given by Vinnikov et al. (1996) with the following conclusions. The results show that the interannual variability of total soil moisture does not seem to differ significantly between each one of the catchment sites. Observations of water-table depths would seem to suggest the forest catchment shows slightly less interannual variability than the grassland and growing forest catchments. Looking at the runoff results, it appears that runoff in the grassland catchment is always higher than in the forest and has more interannual variability, as might have been expected. But in the growing forest catchment, the runoff first parallels the grassland from 1960 to 1970, showing that these measurements are indeed representative, then parallels the forest for 5 years (1971–75). For the last 10 years (1976–85), the growing forest's runoff is less than the mature forest's, which would suggest that the growing forest is utilizing additional water to mature the canopy.

In 1975, the annual averaged values of total soil moisture and depth of the water table are at their lowest and deepest, respectively. This would suggest that a significant drying event had occurred. The monthly observations (Fig. 3) reveal the dramatic drying period during the summer of 1975 with a very deep water table, very dry soil moisture stores, and no runoff during the latter part of the year. In addition, a fairly robust summer drying is also seen to occur during 1972. The dry conditions of the warmer months of 1972 and 1975 seem to be preceded by one or more months with below normal precipitation between January and May. In addition, a very shallow winter snowcover occurs in 1972.

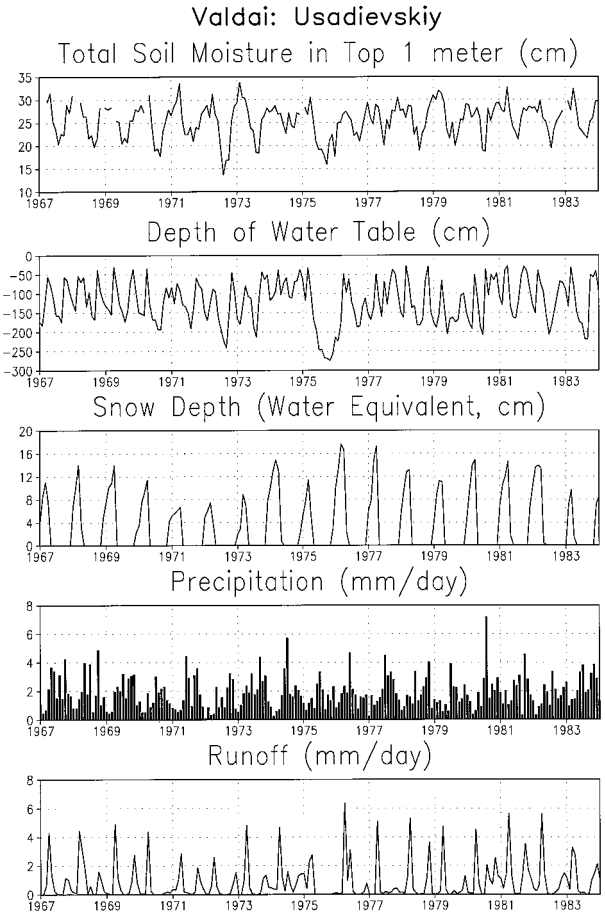

FIG. 3. Monthly observations for the years 1967–83 of total soil moisture, water-table depth, snow depth (water equivalent), and runoff for Usadievskiy. Shown also are monthly observations of precipitation. Tick-mark labels correspond to January of the indicated year.

b. Meteorological data

Routine observations of standard meteorological variables have been made at the Valdai research site for a number of years (Table 1). The collection of meteorological data used in this study spans a time period of 1966–83. The meteorological instruments used to obtain this data were located on a natural grassland plot. These observations were taken at 3-h intervals, eight times per day (0000, 0300, 0600, 0900, 1200, 1500, 1800, and 2100 local time) and include the following meteorological variables needed as forcing for the land-surface model simulations: T_a air temperature at standard level of measurement (°C), T_d dewpoint temperature at standard level of measurement (°C), P precipitation (mm), C_L lower cloud-cover fraction, C_T total cloud-cover fraction, V wind speed at standard level of measurement (m s^{-1}), and p_a sea level pressure (mb). These variables were then used to force the models directly or to supply values to algorithmic arguments used within the models.

An additional set of unique rain gauge data was also utilized in this study. Near the Usadievskiy catchment, monthly totals of precipitation were obtained through the use of a modified rain gauge instrument (gauge 98; Golubev et al. 1995). The rain gauge was designed so that the effects of wind biasing on the catchment of snowfall and rainfall in the gauge were minimized by surrounding the rain gauge with natural shrub-type vegetation. The height of the shrub vegetation was maintained at the same height as the top of the rain gauge. Precipitation totals were recorded twice daily for the years 1974–83. The seasonal cycle of monthly precipitation measured at the rain gauge 98 site, as compared to the precipitation measured at the meteorological instrument site, shows the measurements obtained for rain gauge 98 are higher during the fall and winter months (Fig. 4). This would suggest that the rain gauge at the meteorological site was not capturing as much precipitation as rain gauge 98 due to the aerodynamic effects on wind-blown snow (D. Yang et al. 1995).

Through the use of these rain gauge 98 data, monthly correction coefficients for the precipitation measurements at the meteorological instrument site were calculated in order to correct for wind biasing. Each monthly correction coefficient μ_M is simply the ratio of the rain gauge 98 monthly total to the meteorological rain gauge monthly total, averaged for all the years:

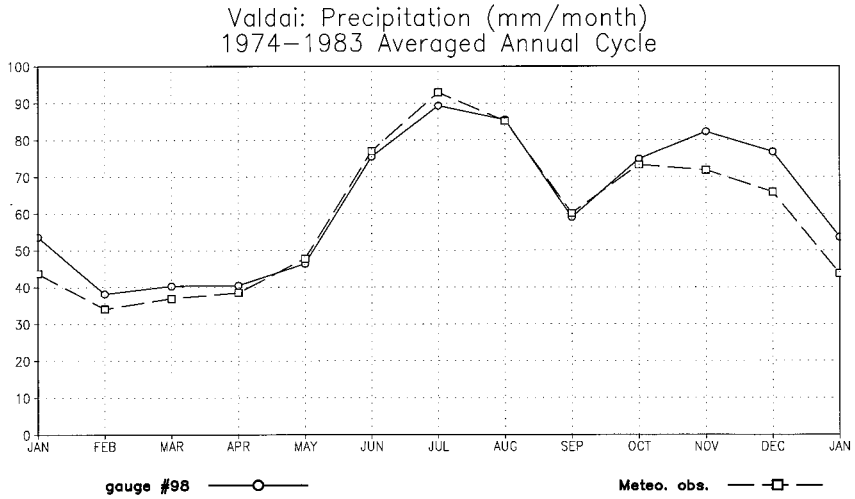

FIG. 4. Seasonal cycles averaged for the years 1974–83 of monthly precipitation measured with rain gauge 98 and the gauge at the meteorological station.

$$\mu_M = \frac{\sum_{1974}^{1983} \frac{P_M^{98}}{P_M^{\text{meto}}}}{10}, \tag{1}$$

where P_M^{meto} is the monthly total precipitation measured at the meteorological site, and P_M^{98} is the monthly total precipitation measured at gauge 98. Correction values are greater than 1 during the fall and winter months and not significantly different from 1 during the spring and summer months (Table 2). Using the appropriate monthly value of μ_M, the result is a ''corrected'' value of the precipitation for each time step, P_C, given by

$$P_C = \mu_M P. \tag{2}$$

c. Evaporation as a residual

Using the monthly observations of soil moisture, runoff, snowcover, and precipitation, a residual estimate of monthly evaporation is possible. By rewriting the basic water-balance equation that describes changes in soil moisture in the top 1 meter of soil,

$$\frac{dW}{dt} = P_R - E + M - R_{1\text{m}}, \tag{3}$$

where W is total soil moisture in the top 1 m of soil, P_R is rainfall (measured precipitation that occurred when $T_a > 0$°C), E is evapotranspiration, M is snowmelt, and $R_{1\text{m}}$ is runoff from the top 1 m of soil, we can obtain an equation for an evaporation residual estimate

TABLE 2. Monthly values of the precipitation correction coefficient μ_M. Note: For the remaining months, $\mu_M = 1.0$.

	Jan	Feb	Mar	Nov	Dec
μ_M	1.2	1.1	1.1	1.1	1.2

$$E = P_R + M - R_{1\text{m}} - \frac{dW}{dt}. \tag{4}$$

Measurements of water equivalent snow depth were taken during measurable snow events, near the end of each month and every few days in the spring during rapid snowmelt. So we calculated monthly snowmelt M as the total observed decrease in water equivalent snow depth within the month. The runoff from the top 1 m of soil $R_{1\text{m}}$ is comprised of the overland runoff R_O and the drainage of groundwater R_D out of the top 1 m of soil:

$$R_{1\text{m}} = R_O + R_D. \tag{5}$$

The monthly runoff measurements made at Usadievskiy reflect the total runoff from the catchment and not from the top 1 m of soil. To account for this inconsistency, variations in observed water-table depth were used. If the water-table depth WT was observed to be deeper than 1 m, a decrease in the depth of the water table was assumed to reflect the drainage coming from the top 1 m layer of soil, R_D, and an increase in the water-table depth was assumed to contribute to catchment runoff (i.e., the observed runoff). Changes in water-table depth were equated to these water fluxes by an empirical constant μ_W. When the water table was observed to be in the top 1 m of soil, the total catchment runoff R was assumed to be representative of the runoff from the top 1 m of soil:

$$R_{1\text{m}} = \begin{cases} R - \mu_W \dfrac{d\text{WT}}{dt}, & \text{WT} > 1 \text{ m} \quad (6) \\ R, & \text{WT} < 1 \text{ m}. \quad (7) \end{cases}$$

Through empirical evidence and basic soil physics arguments, the most appropriate value for μ_W is 0.1 (Fedorov 1977).

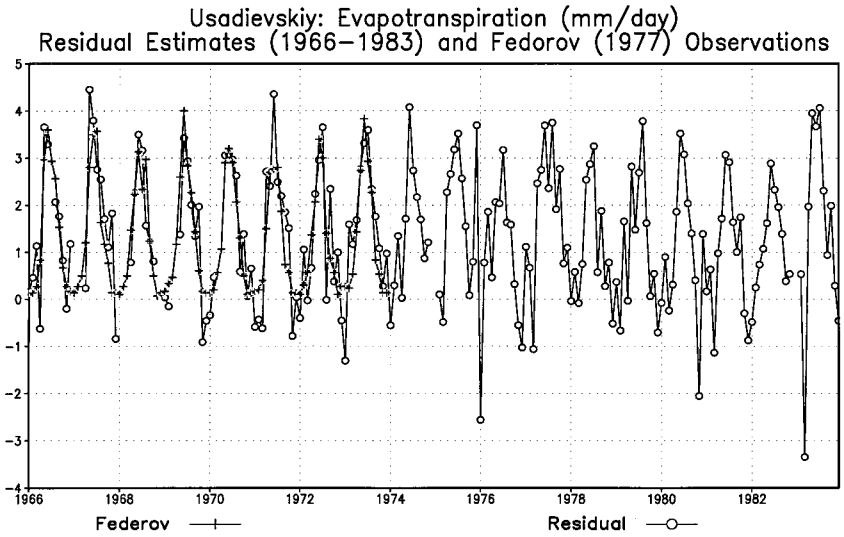

FIG. 5. Monthly evaporation estimates using a residual calculation for the years 1966–83 and observations from Federov (1977) for the years 1966–1973 at Usadievskiy catchment.

The calculated residual evaporation shows a well-defined seasonal cycle with a summer maximum, as one would expect (Fig. 5). However, the residual calculation also produces negative values of evaporation, especially during the winter months, and these values are most likely erroneous.

Evaporation measurements and estimates for the Usadievskiy catchment were also made by Fedorov (1977) from 1960 to 1973 (Fig. 5). During the warmer months, May through October, weighing lysimeters were used to measure monthly evaporation within the catchment. For the remaining months, November through April, an estimate of evaporation was calculated using the Budyko (1956) algorithm for potential evaporation estimates. A good agreement in the seasonal cycles between the residual and the Fedorov estimates is seen during the warmer months (Fig. 6). However, the observations show a fair amount of disagreement during the fall and winter months. The residual estimate appears to be systematically higher than the Fedorov measurements during the months of September and October. This is likely caused by the high amounts of rainfall that were measured (Fig. 6).

Nonetheless, the relative agreement between the Fedorov observations and the residual estimates of evaporation during the summer months, when evaporative fluxes are most significant, is encouraging. In light of the likely erroneous negative values during the winter

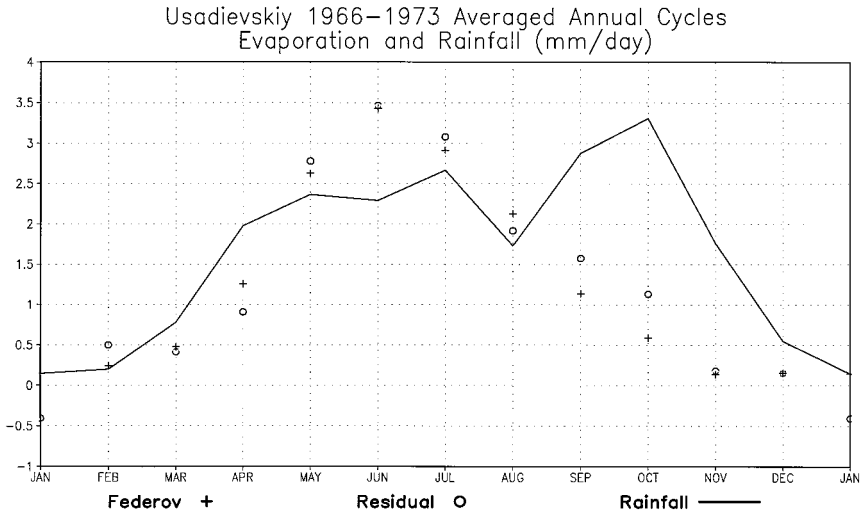

FIG. 6. Seasonal cycles averaged for the years 1966–73 for evaporation estimates at Usadievskiy from Fedorov (1977) and from residual calculations. The seasonal cycle (1966–73) of rainfall used in the residual calculations is also shown.

months and the slight bias during the fall of the residual calculations, the Fedorov estimates are likely the better choice to use as ''observations.'' However, both the Fedorov estimates and the residual calculations will be used in the validation analysis of the model simulations (section 4).

d. Radiation data

The data obtained from the Valdai research site did not include any downward longwave measurements. In order to force the models, an algorithm was needed to simulate the incoming longwave radiation. The results from Brutsaert (1982) show the Satterlund (1979) scheme to be the best algorithm for estimating clear-sky downward longwave radiation (especially for subfreezing air temperatures). In addition, results from the RO study show that models forced with the Satterlund scheme agree well with observations in their simulation of net radiation. As a result, the Satterlund scheme was used for the simulations to provide an effective estimate of incoming longwave radiation. Recently, other studies (e.g., Yang et al. 1997; A. Pitman 1996, personal communication) have chosen the Idso (1981) longwave algorithm. However, our sensitivity analysis (not shown) reveals only slight differences between the simulations of both the bucket and SSiB models result using the two different longwave algorithms. To adjust for cloudy conditions, the Monteith (1961) formula was used with some slight modifications (refer to RO for a complete description).

Measurements of shortwave radiation were made at Valdai during the growing season but were halted during the winter due to the extreme freezing conditions. In addition, the shortwave observations were supplied in 10-day averaged diurnal cycles, rather than the routine format of the meteorological data (every 3 h). As such, the shortwave radiation data were inappropriate to use as forcing for the models and an additional algorithm was needed to simulate incoming solar radiation. Using the data from the RO study, Schlosser (1995) compared simulations of incoming solar radiation with an algorithm developed by Berlyand (1956) and Berlyand (1961) to the observations. In addition, test simulations of the bucket and SSiB models for each of the stations using the solar algorithm as forcing rather than observations show that Berlyand's algorithm is quite suitable to be used as solar forcing for these simulations. The algorithm also agrees well with the observations at Valdai (Fig. 7), and their differences are well within the 20 W m^{-2} instrument error (Vinnikov and Dvorkina 1970) of the Yanyshevski pyranometer used to measure the solar radiation. The algorithm was also able to reproduce the observed diurnal structure of solar radiation rather well (not shown). In light of these results, the Berlyand algorithm is quite suitable for the Valdai simulation experiments.

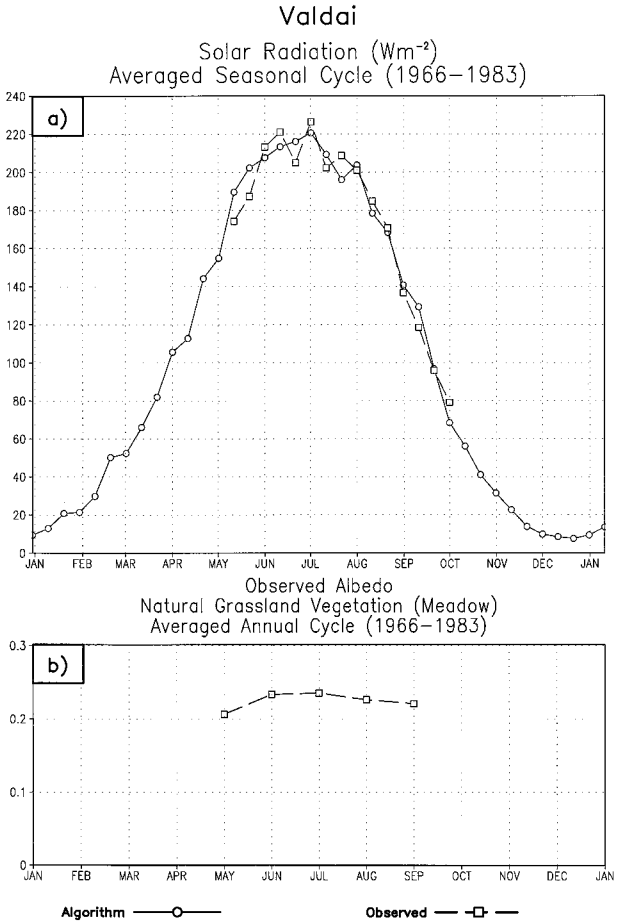

FIG. 7. Seasonal cycles (1966–83) of (a) observed solar radiation and simulated solar radiation at Valdai using the Berlyand (1961) algorithm and (b) observed albedo for a natural grassland vegetation (meadow) plot at Valdai.

3. Models

The two models used for this study are the simple bucket hydrology model (Budyko 1956; Manabe 1969) and the SSiB model (Xue et al. 1991). Some slight modifications to both of the models were made for the Valdai simulations based on the results of RO and Schlosser (1995). These modifications are discussed below and summarized in Table 3. The simple bucket hydrology framework is still widely used for land-surface parameterization in GCMs, and the SSiB model represents the recent efforts to provide more sophisticated and explicit parameterizations of land-surface processes for GCM applications. So it is useful to examine the mechanisms of the models' seasonal and interannual hydrologies, which differ in complexity, to each other and to the Valdai observations.

a. Model hydrologies

The bucket hydrology provides a simple representation of the plant-available soil-water budget in the top 1 m of soil using one soil layer storage term:

TABLE 3. Modifications to bucket and SSiB models.

Bucket model
Albedo for grassland set to 0.23 (default value is 0.18 for no snow cover)
Deep snow albedo set to 0.75 (default value is 0.6)
Bucket capacity set to 15.6 cm of plant-available soil moisture (default value is 15 cm)
Potential evaporation correction (Milly 1992)
SSiB model
Porosity set to 0.401 (default value is 0.42 for grassland)
New runoff scheme implemented (Milly and Eagleson 1982)
Large-scale basin flow algorithm turned off
Monthly albedo shifted during growing season
May = −0.008
June = +0.012
July = −0.002
August = −0.078
September = −0.06
Snow albedo set to 0.75 (default value is 0.6)
Wilting level parameter c_1 set at 6.44 to match observed wilting levels of the top 1 m of soil (default value is 5.8)
Middle soil layer thickness set to 98 cm (default value 47 cm for grassland)

$$\frac{dW_a}{dt} = P_R - E_b + M_b - R_b, \tag{8}$$

where W_a is available soil moisture in the top 1 m of soil, E_b is bucket evapotranspiration, M_b is bucket snowmelt, and R_b is bucket runoff. The bucket runoff R_b as originally formulated by Budyko (1956), consists of an overland flow component, where a fraction of rainfall immediately runs off, and a drainage component (bucket overflow). However, for the Valdai simulations we chose the typical GCM bucket assumption of no instantaneous runoff from rainfall. The bucket will, therefore, only produce runoff when it is saturated (at field capacity) and the infiltrated precipitation is assumed to drain rapidly. The bucket evapotranspiration is given by

$$E_b = \beta E_p, \tag{9}$$

where $\beta = W_a/0.75W_{fc}$ is soil moisture stress to evapotranspiration, $\beta \leq 1$. When snowcover is present or the ground temperature is below freezing, no changes of soil moisture are allowed. Any precipitation that falls in the form of rain is runoff, and evaporation is taken from the snowcover (at the potential rate). The budget equation for the snowcover is then

$$\frac{dW_{sb}}{dt} = P_s - E_p - M_b, \tag{10}$$

where W_{sb} is water equivalent snow depth and P_s is snowfall (precipitation that falls when $T_a \leq 0$°C).

The SSiB model hydrology scheme contains three soil layers and a canopy layer. The budget equation for the canopy water storage is given by

$$\frac{dW_c}{dt} = P_c - D - E_c, \tag{11}$$

where W_c is canopy interception water store, P_c is precipitation intercepted by the canopy, D is drainage rate, and E_c is evaporation of canopy water store. For SSiB's three soil layers, the water budgets can be expressed as

$$\frac{dW_1}{dt} = P_i - Q_{12} - E_{bs} - r_1E_t - R_s \tag{12}$$

$$\frac{dW_2}{dt} = Q_{12} - Q_{23} - r_2E_t \tag{13}$$

and

$$\frac{dW_3}{dt} = Q_{23} - Q_3 - r_3E_t, \tag{14}$$

where W_i is total soil moisture in the ith soil layer, P_i is precipitation infiltration, Q_{ij} is water flux between the ith and jth soil layers (positive denotes a downward flux), E_{bs} is bare soil evaporation rate, E_t is transpiration rate, R_s is surface runoff rate, Q_3 is drainage rate from the lowest soil layer, and r_i is root-distribution factor for the ith soil layer. When the top soil layer is unsaturated, P_i is equal to the precipitation that was not intercepted by the canopy (throughfall) and $R_s = 0$; upon saturation, any excess precipitation is assumed to be surface runoff R_s. The interlayer water flux terms are calculated by solving for the diffusion equation using the finite-difference method. During frozen soil conditions the infiltration rates, interlayer water fluxes, and drainage rates are diminished by decreasing the mean hydraulic conductivity of each soil layer linearly with soil temperature (described in a later section). A detailed description of each of the terms in (12)–(14) is given by Xue et al. (1996a). The budget equation for SSiB's water equivalent snow depth W_s is given by

$$\frac{dW_s}{dt} = P_s + F - M_s - E_s, \tag{15}$$

where M_s is snowmelt, F is freezing of water on canopy, and E_s is evaporation from snow. Any water stored on the canopy that freezes is added to the water equivalent snow depth [the F term in (15)]. Similar to the bucket framework, during snowcover conditions SSiB does not allow any evapotranspiration from the soil layers. It should be noted that the E_s term was erroneously left out in the text of Xue et al. (1996a).

b. Bucket model modifications

The RO study found that for some of the station cases, the bucket model was limited in its soil moisture simulations by the assumed 15-cm capacity of its plant-available soil moisture store (hereafter referred to as plant-available field capacity). Sensitivity tests of Schlosser (1995) with the bucket model using observed plant-available field capacities of the RO stations showed significant improvements to the simulations. In light of these results, the field capacity of the bucket

TABLE 4. Soil characteristics at Usadievskiy. Coverage and water-holding characteristics for each soil type (Fedorov 1977). Percent coverage is based upon areal coverage within the catchment, $W*$ is the wilting level of the top 1 m of soil, W_f is the field capacity of the top 1 m of soil, and W_0 is the total water-holding capacity of the top 1 m of soil. Catchment averages are weighted with respect to percentage of soil-type area coverage.

Soil type	Loam	Sandy loam	Sandy	Catchment average
Percent coverage	56	28	16	
$W*$ (cm)	13.4	10.9	5.8	11.5
W_f (cm)	30.8	25.3	17.5	27.1
W_0 (cm)	37.4	44.7	41.2	40.1

model was adjusted for the Valdai simulations. An average field capacity for the Usadievskiy catchment was calculated using observations of soil type coverage over the catchment and measurements of field capacity and wilting level available from Valdai for the different soil types.

Table 4 lists the measurements obtained for each soil type and the catchment averaged values of total water holding capacity W_0, field capacity W_f, and wilting level W_*, for Usadievskiy (Fedorov 1977). The averaged field capacity estimate for Usadievskiy is 27.1 cm and the averaged wilting level is 11.5 cm. Field capacity and wilting level measurements were taken according to a standard technique designed for the Russian water-balance station network. Field capacity is measured by saturating a covered and enclosed plot of soil (in order to prevent evaporation loss and lateral movement of soil water, respectively) and monitoring the decay of rapid drainage from the soil. The wilting level is calculated on an agricultural plot using an oat crop. Vinnikov and Yeserkepova (1991) give a more detailed explanation of these measurement techniques. Since the bucket model simulates plant-available soil moisture, W_* is subtracted from W_f to obtain an appropriate field capacity for the bucket model of 15.6 cm. When comparing with observations of total soil moisture, W_* is then added back to the bucket's simulated available soil moisture to produce a bucket total soil moisture.

Sud and Fennessy (1982) and Milly (1992) noted an inconsistency in the bucket model parameterization of potential evaporation used in GCMs. For the Valdai simulations, the bucket model was modified to correct for this inconsistency so that the potential evaporation rate E_p was calculated for the surface temperature at completely saturated soil conditions (rather than for the actual surface temperature):

$$E_p = \rho C_D |V| (q_{ts}^* - q_a), \tag{16}$$

where ρ is air density, C_D is drag coefficient, $|V|$ is wind speed at standard measurement height, q_{ts}^* is specific humidity of air temperature of a saturated surface, and q_a is specific humidity at standard level of measurement. We use the standard value of C_D ($=0.003$) equal to that of the GFDL GCM for all surfaces (RO) and within the acceptable range of values for grassland vegetation (Hartmann 1994). It should be noted that the value of C_D, which partly depends upon the roughness of the canopy surface (Stull 1991), can be varied according to observations of a particular site (as in Chen et al. 1997) or to more consistently represent a smoother or rougher vegetation. So in theory, the bucket model can represent a wide range of vegetation types in its heat flux parameterization.

Finally, the bucket model albedo was adjusted for the Valdai simulations. Observations of albedo for a meadow (i.e., natural grassland vegetation) plot at Valdai were taken for the years 1966–83 during the warmer months. These observations were then used to adjust the bucket's albedo. The standard bucket assumes a value of 0.18 (RO). Figure 7 gives an averaged seasonal cycle of the albedo measurements during the growing season. The observed albedo has an average value for the growing season of approximately 0.23. The standard bucket scheme assumes a constant value, thus the observed monthly variations of albedo (Fig. 7) cannot be reproduced. As such, the bucket's albedo was set to 0.23 as the best approximation. Unfortunately, no observations of albedo during snowcovered conditions were made at Valdai. However, the results of the RO study suggest that the standard bucket snow albedo is too low for off-line simulations of natural grassland vegetation (Fig. 14 of RO). Using the observations of the RO study, a snow albedo of 0.75 was prescribed to the bucket model for the Valdai simulations.

c. SSiB model modifications

The results of the RO study suggested that during the springtime SSiB showed an inconsistent partitioning of snowmelt into runoff (Fig. 8 of RO). In light of these results, a new runoff scheme was tested with SSiB. The new runoff scheme includes modified mean hydraulic conductivity calculations that are based upon the parameterizations of Milly and Eagleson (1982). This runoff scheme is also included in the latest test version of SiB2 (Sellers et al. 1996). The most notable difference from the original runoff scheme is during frozen soil conditions. The mean hydraulic conductivity K_{av} is decreased to limit the infiltration of snowmelt, interlayer exchanges of soil moisture, and gravitationally driven drainage. The mean hydraulic conductivity for frozen soil conditions K_{frz} is given by

$$K_{\text{frz}} = F_{\text{adj}} K_{\text{av}}, \tag{17}$$

where

$$F_{\text{adj}} = \begin{cases} \dfrac{T_{\text{soil}} - 263}{10}, & 263 < T_{\text{soil}} < 273 \\ 0, & T_{\text{soil}} \le 263 \end{cases} \tag{18}$$

and

$$T_{\text{soil}} = \begin{cases} T_s, & \text{infiltration and upper-layer moisture fluxes (K)} \\ T_{\text{deep}}, & \text{lower-layer soil moisture fluxes (K).} \end{cases}$$

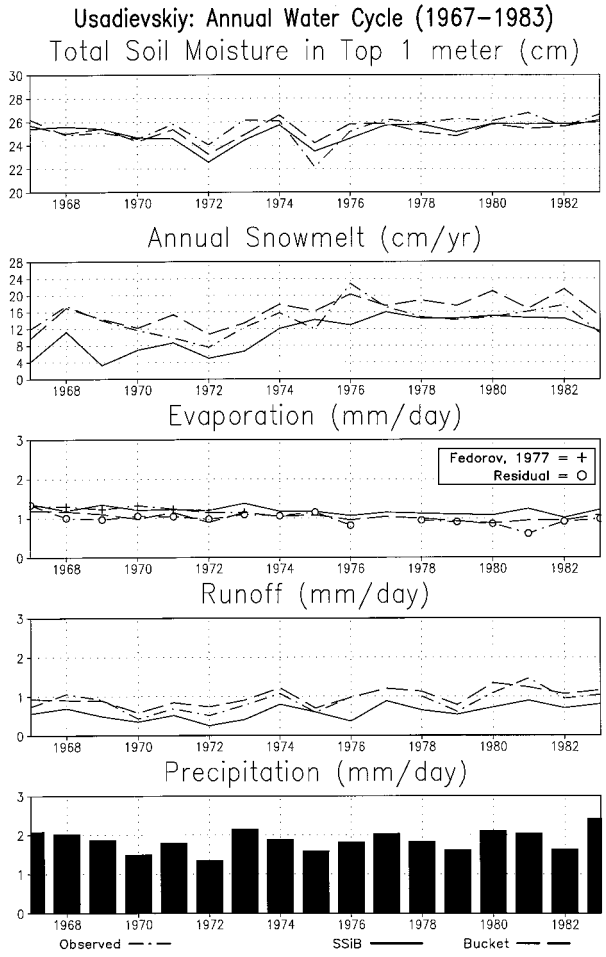

FIG. 8. Annual averaged values of observed and simulated total soil moisture, snowmelt, evaporation [observed residual denoted by an open circle and (Fedorov 1977) by a crosshair], and runoff for the years 1967–83 at Usadievskiy. For the residual evaporation estimates, (4) was used with annual values for the right-hand-side terms. In addition, the annual averages of observed precipitation are given.

Here, T_{deep} is the deep soil temperature. This algorithm replaces the rather simple criteria of the original runoff scheme where no snowmelt infiltration, interlayer soil moisture exchanges, and drainage are allowed if the deep soil temperature is below freezing. With the new runoff scheme, SSiB's soil moisture during the springtime shows a more realistic peak as seen in the observations for four of the six RO stations (Xue et al. 1996a). While the test results of SSiB are not conclusive, it does appear that the new runoff scheme of SSiB shows an improved simulation of runoff partitioning during the springtime. As a result, the new runoff scheme was chosen to be used for the SSiB simulations of Valdai.

Another slight modification was made to SSiB's runoff parameterization. An empirical algorithm used to simulate large-scale river baseflow was turned off since the Valdai simulations were for a much smaller scale (a catchment).

In the RO study, the standard GCM values for a grassland vegetation physiology were used. However for the Valdai–Usadievskiy simulations, a few of these parameter values were replaced with observed values. The area-averaged total water-holding capacity (i.e., porosity) of the top 1-m of soil was estimated to be 40 cm (Table 4). So a soil porosity of 0.40 for the catchment was used in place of the standard porosity value for grassland of 0.42. In addition, SSiB's wilting level was adjusted to fit observations. Following the relationship described in detail by Xue et al. (1996a), we adjusted SSiB's wilting level parameter, c_1, to match the wilting level for the top 1 m of soil at Usadievskiy. The new and default values of c_1 are given in Table 4. SSiB has no explicit field capacity parameter to set to observations, but rather a drainage term that varies exponentially with soil wetness (Xue et al. 1991). Using the method described by Xue et al. (1996a), we find that when we set SSiB's soil moisture stores equal to the observed field capacity of the catchment (Table 4), the SSiB drainage rate becomes very small (less than 0.25 mm day^{-1}), and so SSiB is essentially at its field capacity as well. Thus, no further parameter modifications were needed to adjust SSiB's implied field capacity.

For the remaining soil and vegetation parameters that could not be assigned observed values, the standard GCM values for grassland vegetation type were used. These standard GCM values of the parameters fall within the realistic range of values for the observed soil and vegetation types of the catchment (Table 4). However, the values of soil parameters, such as saturated hydraulic conductivity, are not a function of vegetation type (as is done for SSiB in a GCM) and can vary by orders of magnitude for a given soil type (Domenico and Schwartz 1990). In addition, the lack of observations and the resulting uncertainties for some of the vegetation parameters such as the leaf area index (LAI) can have an impact on SSiB's evaporation calculations (Xue et al. 1996b). We performed sensitivity runs and found that SSiB's latent heat flux calculation is sensitive to changes in LAI for the Valdai simulations. The results of these tests will be discussed in the concluding section of the paper.

SSiB's simulations of soil moisture will be compared with measurements of total soil moisture made in the top 1 m of soil. As a result, SSiB's soil layer depths were modified so that its top two root-active layers were contained in the top 1 m of soil. Only the middle soil layer thickness was changed from the standard value of 0.47 to 0.98 m. The top and bottom layer thicknesses were kept at their standard values of 0.02 and 1.00 m, respectively.

SSiB's albedo was also adjusted according to observations. However, the vegetation parameter values were not modified, as quite a few vegetation parameters can affect SSiB's albedo calculations such as greenness, LAI, vegetation cover fraction, leaf angle distribution, and reflectances. Thus, it would be difficult to choose

TABLE 5. Statistics of observed and simulated hydrologies. Averages and standard deviations for the years 1967–83. Standard deviations are computed using annual means (Fig. 8). For evaporation, light font indicates statistics computed for the years 1967–83 (observations are the residual estimates), and the bold font indicates statistics computed for the years 1967–73 [observations are the Fedorov (1977) data].

	Total soil moisture (cm)	Evaporation (mm day^{-1})	Runoff (mm day^{-1})
Observed	25.5 ± 1.1	1.0 ± 0.2	0.8 ± 0.3
		1.2 ± 0.04	
Bucket	25.2 ± 0.8	1.0 ± 0.1	1.0 ± 0.2
		1.1 ± 0.07	
SSiB	25.1 ± 0.9	1.2 ± 0.1	0.6 ± 0.2
		1.3 ± 0.08	

which parameter to modify, especially when no observations of these values were made at Valdai. Instead, a subroutine was constructed, which would shift the calculated albedos by a prescribed constant value for each month. Using the standard values of vegetation parameters for grassland, SSiB's albedos were calculated and then compared to the observations shown in Fig. 7. Monthly albedo adjustment values were prescribed so that SSiB's albedos matched the observations (Table 3). For snowcover, SSiB's snow reflectances were set to 0.75 according to the observations of the RO stations.

d. Spinup of models

A set of simple experiments, similar in design as described by Z. L. Yang et al. (1995), was performed with the data of the RO study in order to provide a more thorough assessment of the bucket and SSiB models' inherent spinup for off-line simulations using the Russian data (Schlosser 1995). The specific findings of these tests are beyond the scope of this paper. However, the overall results suggest that all simulation biases due to the initialization can be removed for the bucket and SSiB models if they are allotted a spinup integration period of 1 year and their soil moisture stores initialized as completely saturated. In light of these results, the Valdai simulations begin at 1966 with completely saturated soil moisture stores. The simulated output from 1967 to 1983 of the integration is then used to compare with observations.

4. Evaluation and intercomparison of model simulations

a. Annual means and interannual and seasonal variability

Generally speaking, the models do reasonably well at simulating the observed averaged hydrology over the simulation period and the interannual variability (Table 5). However, while both models show the soil moisture drying in 1972 and 1975 similar to the observations, the observations show 1975 as the driest year and the models have 1972 as the driest year (Fig. 8). The largest disagreement between the models' simulated annual averaged total soil moisture in the top 1 m and the observations occurs during the years when their annual averages are most variable (1971–76). SSiB also tends to produce less annual snowmelt (i.e., lower snow depths) and runoff with respect to observations and the bucket. The reason for SSiB's snowmelt discrepancy is discussed in the seasonal cycle analysis. The bucket model tends to produce higher amounts of annual runoff than both the observations and SSiB. In 1977, the observed runoff rates for Usadievskiy during the fall are inconsistently low with respect to the runoff of the other two catchments (not shown) and to the high precipitation rates (Fig. 3), and thus appear questionable. As a result, the observed runoff was omitted from the interannual analysis (Fig. 8 and Table 5).

Qualitatively, both the models and observations show similar traits for their seasonal cycles of total soil moisture, snowdepth, evaporation, and runoff (Fig. 9). Soil moisture is at its lowest during the summer months and is replenished during the fall. The models and observations also agree fairly well on the magnitude of the summer drying of the soil. Evaporation is at its maximum during the summer. Runoff peaks during the spring snowmelt. Closer inspection however reveals notable differences between the modeled and observed seasonal variability. The bucket tends to make July the driest month, while observations show August as the driest month on average. SSiB's summer drying of the soil agrees with the bucket. Another notable disagreement is seen during the spring snowmelt. Observations show the soil moisture on average to peak above its catchment averaged field capacity of 27.1 cm (Table 4). The bucket model simulation keeps its soil moisture at field capacity on average from late fall into early spring with no peak occurring due to the snowmelt. Similarly, SSiB's soil moisture appears to be fairly constant at just below the bucket and observed field capacity from late fall to early spring.

The bucket model's soil moisture is limited by its field capacity and thus cannot reproduce the observed spring peak of soil moisture. Since the bucket has less soil moisture than the observations in the spring and the highest evaporation rate with respect to SSiB and the observations in May (Fig. 9), it is able to dry out quicker during the ensuing summer.

SSiB, in theory, can account for the observed spring behavior of soil moisture and groundwater. Observations reveal that the water-table depth rises above 1 m every year during the springmelt (Fig. 3). To be consistent with observations, SSiB's lowest soil layer should be saturated (i.e., wetness is equal to 1.0) during the spring snowmelt. However, on average SSiB's lowest soil layer is not saturated (Fig. 10) and this will cause soil water from SSiB's upper layers to drain rapidly (by gravity). As such, the quick drainage of soil water from SSiB's upper layers during the snowmelt

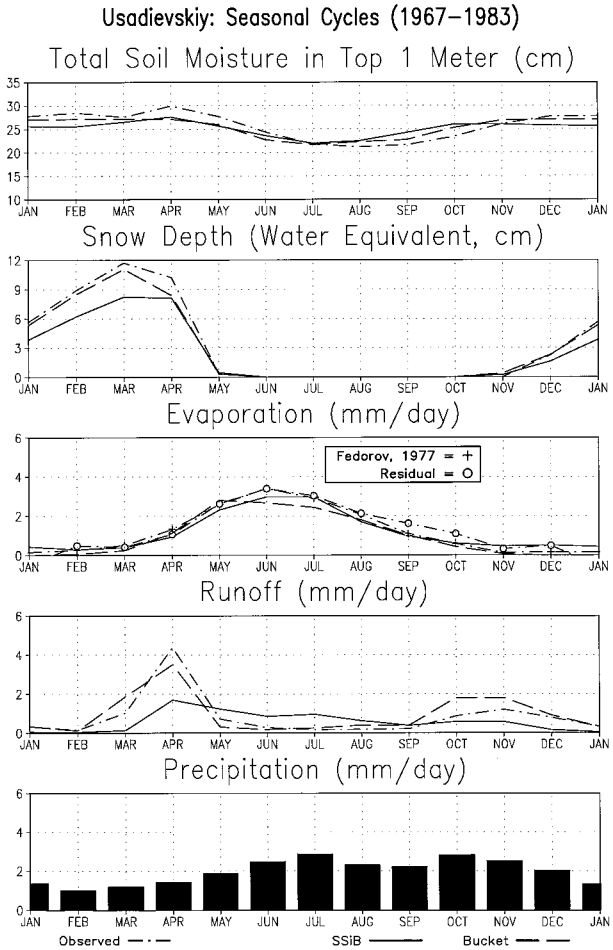

FIG. 9. Seasonal cycles of observed and simulated total soil moisture, snow depth (water equivalent), evaporation (residual calculation), and runoff for the years 1967–83 at Usadievskiy. In addition, the seasonal cycle of observed precipitation (1967–83) and the seasonal cycle of observed evaporation from Fedorov (1977) for the years 1967–73 is given.

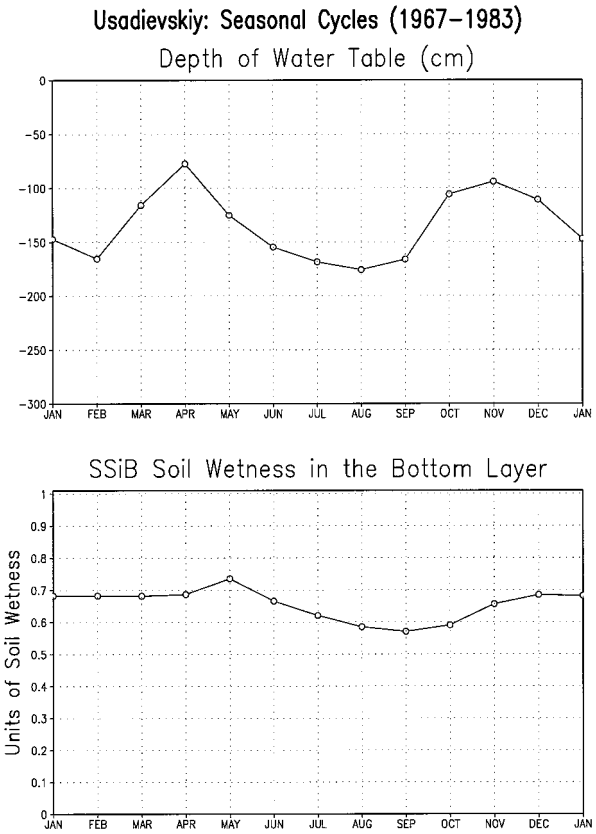

FIG. 10. Top frame: seasonal cycle for the years 1967–83 of water-table depth observations for the Usadievskiy catchment. Bottom frame: seasonal cycle for the years 1967–83 of SSiB's simulated soil wetness in its lowest layer.

makes it difficult to maintain total soil moisture in its top two layers above field capacity (Fig. 9).

Differences between the modeled and observed hydrologies are also seen in the seasonal variability of evaporation (Fig. 9). The bucket's evaporation peaks in May, while the observations show evaporation to peak in June. SSiB's evaporation peak appears to extend through June and July. In addition, the magnitude of both modeled peaks in evaporation is lower than the observed peak. The bucket's earlier peak in evaporation could be a result of its soil moisture store drying out earlier in the summer, which causes its soil moisture stress to become high and limit evaporation for the remaining summer months. The models tend to agree with the Fedorov observations during the fall rather well, and the higher residual observations are likely a result of its fall bias described earlier (Fig. 6). In addition, SSiB produces more evaporation than the bucket from late fall into early spring.

For runoff, both the models and observations on average show a runoff maximum associated with the spring snowmelt. In March, the bucket model shows the largest decrease of snowcover and thus the highest amount of runoff, since the bucket is at saturation (Fig. 9) and all of its snowmelt goes into runoff. In April, the observations have the highest amount of snowmelt (Fig. 9) and a water-table depth less than 1 m (Fig. 10), so the higher runoff rates than the models would be expected. During the summer, SSiB tends to produce more runoff than both the bucket and observations. This discrepancy is caused by the drainage term, Q_3, from its bottom soil layer (14) and not by surface runoff (12), as W_1 is always well below saturation during the summer for the Valdai simulations (not shown). The bucket runoff rates tend to agree rather well with observations from late spring to early fall. During the late fall, the bucket produces the highest amount of runoff due to increased precipitation and a saturated soil moisture store. It is difficult to determine whether SSiB or the bucket produces a better runoff simulation during the fall. In the

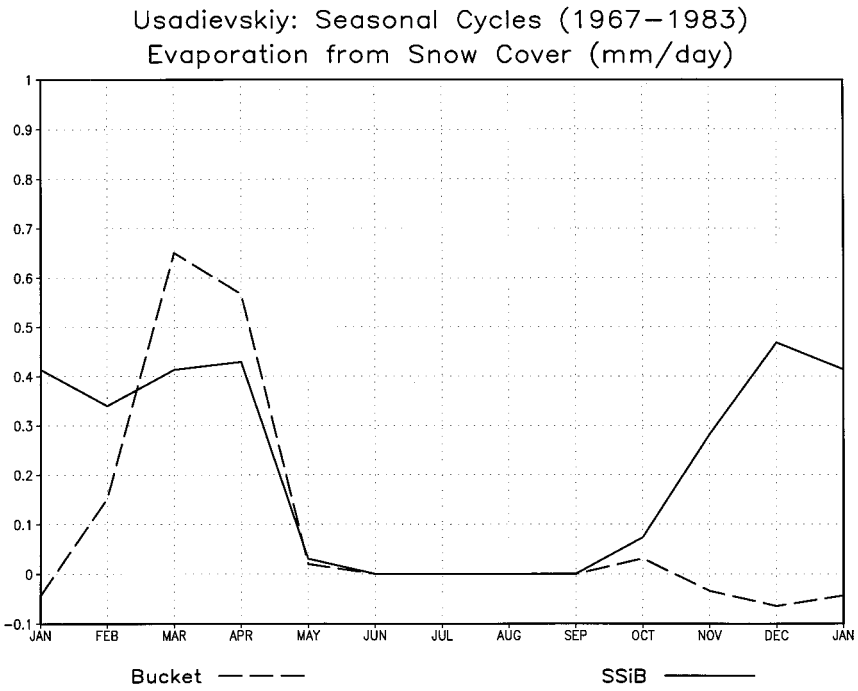

FIG. 11. Seasonal cycles (1967–83) of simulated evaporation from the snow cover for the bucket and SSiB models.

winter, both the modeled and observed runoff rates are low and in good agreement.

On the average, the bucket model produces a better simulation of snow depth than the SSiB model (Fig. 9). While both models tend to underestimate the snowcover, SSiB's low bias appears significant and may be the cause of SSiB's low runoff rates during the spring snowmelt. The snow depth simulation results are similar to the findings of the RO study. We have determined that SSiB's lower snow depths are a result of the high amounts of evaporation from the snow surface produced in the winter (Fig. 11). In our preliminary results, lower evaporation rates from the snow surface can be achieved not only by tuning SSiB's internal parameterizations but also by decreasing the downward longwave forcing (which is external to the model). However, the test results also show that while a decrease in downward longwave improves the snow depth simulation, SSiB then produces an erroneous delay in the timing of the snowmelt. Nonetheless, the need of a physically consistent modification to correct this feature is uncertain at this time and is still under investigation.

The temporal standard deviations (i.e., interannual variability) of the modeled and observed seasonal cycles (Fig. 12) show notable discrepancies in their interannual variability of soil moisture. Both the bucket and SSiB models show a marked seasonality to their interannual variability of soil moisture. However, the observations show no such seasonality in the interannual variability of soil moisture. The bucket's interannual variability of soil moisture is largest in June and July and becomes almost zero from the late fall to the early spring. However, since the bucket is typically saturated from the late fall to early spring (Fig. 9), one would expect very little interannual variability of soil moisture. However, even for unsaturated conditions during the fall and winter, the bucket's soil moisture variability would also be limited by its assumption of no changes of soil moisture during frozen conditions. SSiB has its maximum interannual variability of soil moisture during August. From the late fall to the early spring, SSiB's variability of soil moisture is low and remains fairly constant, except for a slight peak in March. SSiB's low soil moisture variability during the late fall and winter is a result of its low hydraulic conductivity values during freezing conditions (see section 3), which limit the fluxes of water in and out of its soil layers.

The bucket and the observations seem to be in fair agreement as to the seasonality of interannual variability of evaporation, with higher values during the summer and lower values during the winter (Fig. 12). The observations show a peak in variability in August while the bucket peaks in April and June. SSiB has its highest degree of variability of evaporation during March and May. In addition, SSiB's evaporation has a higher degree of variability than the bucket and observations during the winter.

The seasonality of the interannual variability of simulated and observed runoff corresponds well with the variability of precipitation (Fig. 12). Relative maxima of runoff variability occur during the spring, late summer, and fall. The notable differences are SSiB's low

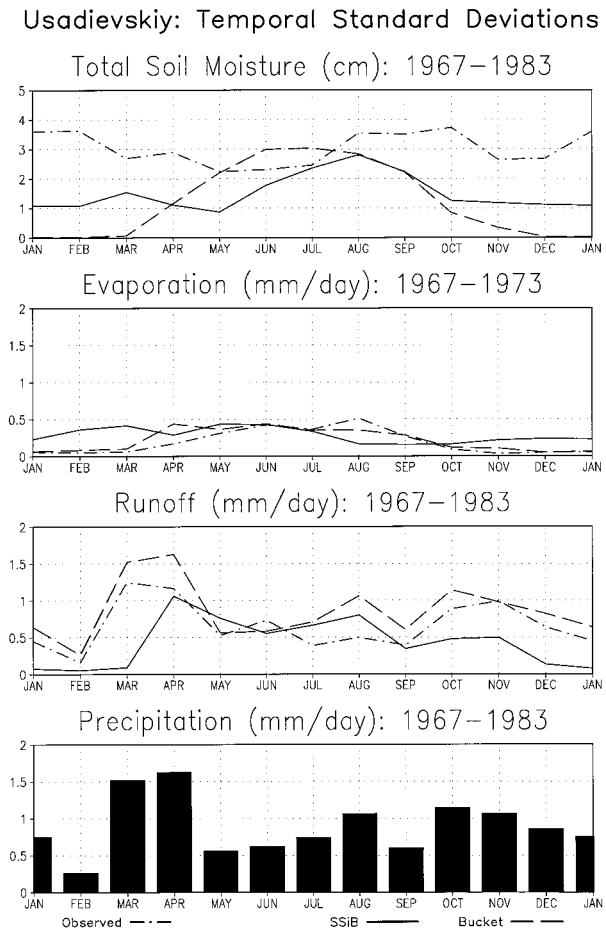

FIG. 12. Temporal standard deviations of the seasonal cycles of observed and simulated total soil moisture, evaporation (Fedorov 1977), and runoff for the years indicated at Usadievskiy. In addition, standard deviations of observed precipitation are given.

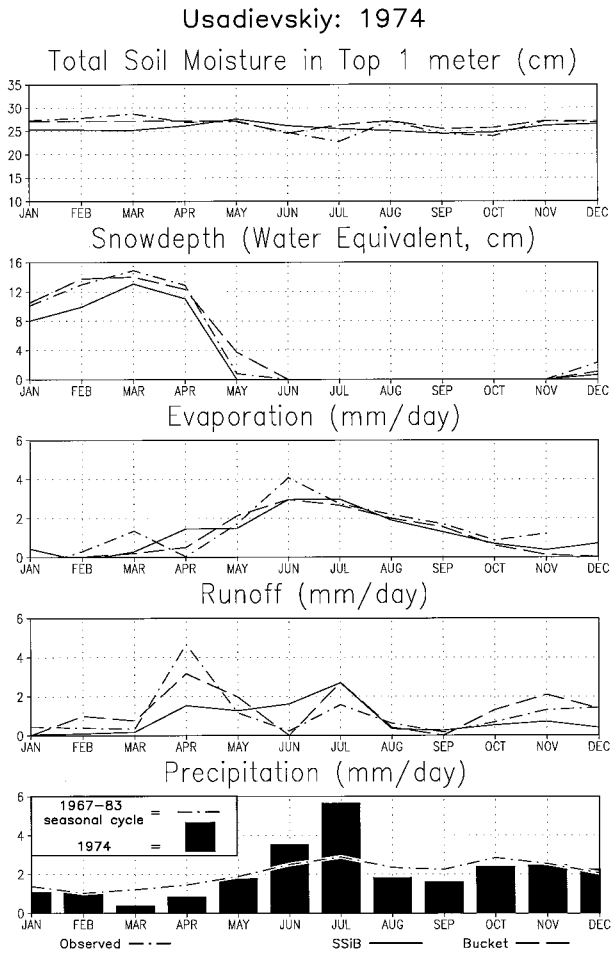

FIG. 13. Monthly results of observed and simulated total soil moisture, snow depth (water equivalent), evaporation (observed residual calculation only), and runoff for the year 1974 at Usadievskiy. Observed monthly precipitation (bars) and the seasonal cycle of precipitation (dotted line) for the years 1967–83 are also given.

variability from October through January, also in March (possibly due to very little snowmelt; Fig. 9), and the bucket's high bias in August and April.

b. Wet years

While 1974 shows no significant increase in annual averaged precipitation (Fig. 8), about twice as much rain fell than the average for July (Fig. 13). As a result, observations show the soil not to dry out as expected during the late summer (Fig. 9) and, in fact, soil moisture increases during July.

The bucket model performs reasonably well at reproducing the observed soil moisture variations during 1974 (Fig. 13), with the slight exception in June. The observations show a decrease in soil moisture, while the bucket tends to increase soil moisture due to a lower evaporation rate. In July, the bucket produces more runoff than observations show. However, the bucket is almost at field capacity for July and so most of the rainfall is partitioned into runoff.

In June, SSiB produces less evaporation but higher runoff rates (from its drainage term) than the observations (Fig. 13), which results in slightly less drying. SSiB, however, simulates a drying of the soil during July, contrary to the bucket and observations, which could be result of its higher runoff (drainage) and evaporation rates than the observations (Fig. 13).

c. Droughts

For the entire time span of the Valdai data, 1972 has the lowest annual averaged precipitation (Fig. 2). In addition, water-table depths averaged over the year are of the deepest of the record. During the summer, the rainfall in June and August was less than half of the average (Fig. 14). After a peak of soil moisture in March, the soil is observed to go through a robust drying period until midsummer when total soil moisture is close to its catchment averaged wilting level (Table 4). The

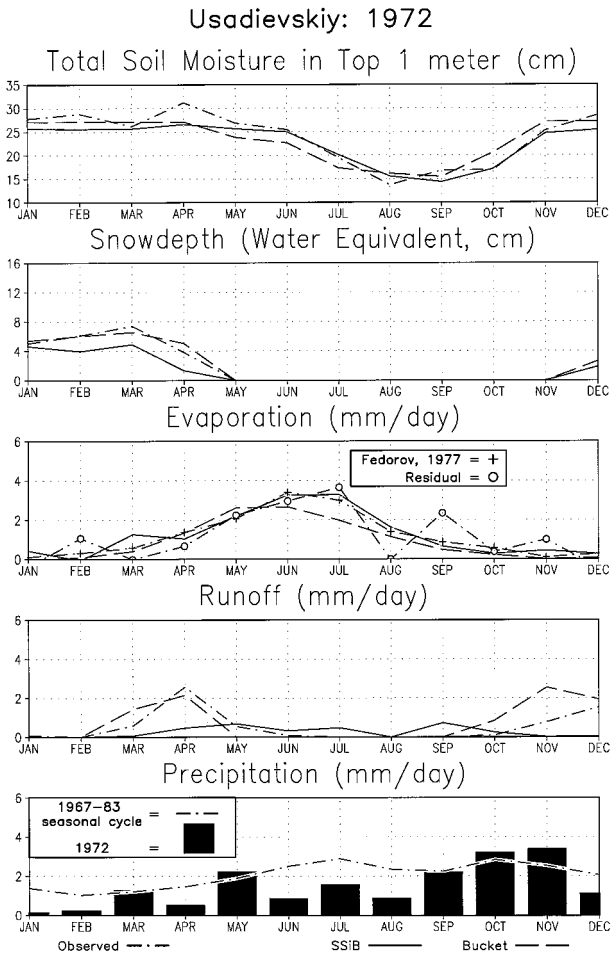

FIG. 14. Monthly results of observed and simulated total soil moisture, snow depth (water equivalent), evaporation (observed residual, denoted by an open circle and (Fedorov 1977) by a crosshair), and runoff for the year 1972 at Usadievskiy. Observed monthly precipitation (bars) and the seasonal cycle (dotted line) for the years 1967–83 are also given.

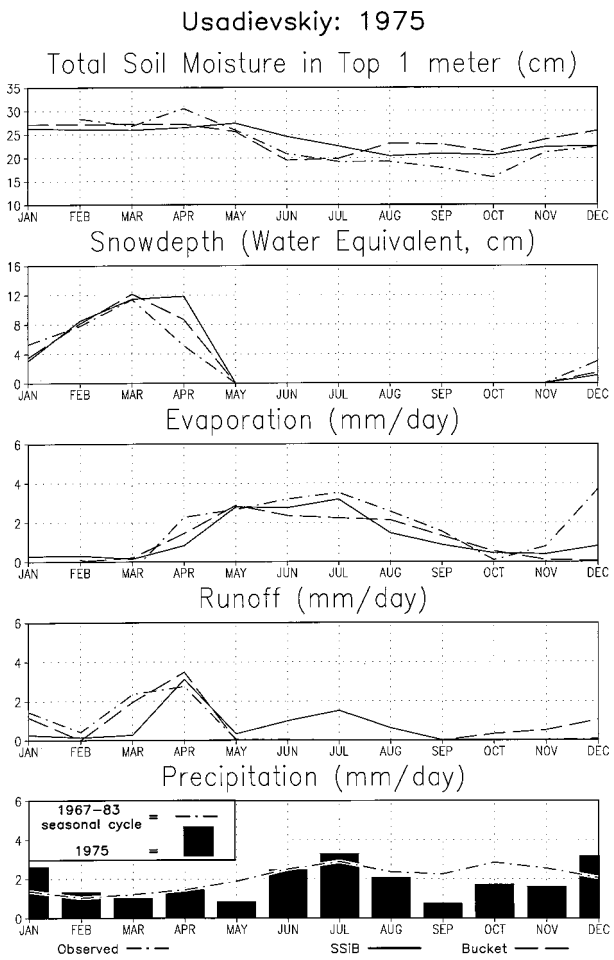

FIG. 15. Monthly results of observed and simulated total soil moisture, snow depth (water equivalent), evaporation (observed residual calculation only), and runoff for the year 1975 at Usadievskiy. Observed monthly precipitation (bars) and the seasonal cycle (dotted line) for the years 1967–83 are also given.

rise of soil moisture observed in August with little rainfall appears questionable. With an increase in soil moisture and little rainfall, the residual estimate of evaporation for August become slightly negative, which is likely erroneous. The Fedorov evaporation observation for August is approximately 1.5 mm day^{-1}.

Generally speaking, both the bucket and SSiB models reproduce the drying of the soil fairly well, but do not reproduce the observed spring peak in soil moisture (Fig. 14). The bucket does a good job reproducing the observed runoff during the snowmelt. SSiB, however, shows no such runoff peak in response to the snowmelt. In fact, nearly all of the snowcover is melted by SSiB a month earlier than the observations and the bucket. After the snowmelt, the bucket's drying is seen to parallel the observations quite well until July, but then the bucket's evaporation decreases considerably, which disagrees with observations. As a result, the bucket's drying diminishes. SSiB tends to dry out the soil a bit more slowly than observed during the early spring. However, from late spring into summer, SSiB's drying parallels the observations quite well.

Much like the year of 1972, the annual averaged precipitation indicates the year of 1975 to be one of the driest years on record for the Valdai data (Figs. 3, 15). In addition, the water-table depth is seen to drop to its deepest level (Figs. 3, 4). A closer inspection reveals that the year of 1975 suffered a significant drought during the fall (Fig. 15). As a result, soil moisture is observed to continue to decrease in September, which normally shows a replenishing of soil moisture (Fig 9).

Looking at the bucket simulation (Fig. 15), soil moisture decreases during September similar to observations. However, a large positive bias of the bucket soil moisture with respect to observations is seen. This bias is a result of a bucket simulation discrepancy that occurs in July. The bucket model shows an increase in soil mois-

ture in July, while the observations show soil moisture to remain fairly constant. The bucket increase in July soil moisture is likely a result of an erroneous simulated evaporation rate that is lower than the observed residual.

SSiB does not seem to reproduce the observed hydrology for 1975 much better than the bucket (Fig. 15). SSiB dries the soil out at a fairly constant rate through July and produces additional runoff in June and July, contrary to the bucket and observations. During the fall drought, SSiB's evaporation rates are lower than observations, and as a result, SSiB does not continue to dry out the soil during the drought. In addition, SSiB produces very little runoff in March due to very little snowmelt, contrary to the bucket and observations.

5. Discussion and conclusions

With 17 years of model simulation (1967–83) and observations of total soil moisture in the top 1 m, runoff, water table, evaporation, and snow depth, the Valdai simulations are the first of their kind to effectively diagnose the interannual and seasonal variability of the land-surface model's simulated hydrologies. Both the bucket and SSiB were improved based on previous results, and the experiments presented here go one step farther in the observationally based validation of these models. From the results presented above, we can reach the following conclusions.

Both the bucket hydrology and SSiB models simulate reasonably well the observed annual average hydrology and its interannual variability. However, the models underestimate the interannual variability of soil moisture during the late fall and winter. This result could be a model inconsistency but also site specific and scale dependent. Further investigation is needed in order to address this issue.

The success of the bucket model and SSiB at reproducing extreme hydrological events is varied. During a drought, both the models were able to produce drier soil conditions, however, the other components of their simulated hydrologies were not accurately simulated. For example, SSiB produced runoff, not seen in the observations, and both the bucket and SSiB models' evaporation rates were low compared to observations. To increase our confidence in coupled GCM climate studies, land-surface models must at least be able to accurately reproduce the hydrological response to precipitation anomalies in off-line tests.

The inability of the bucket model to rise above its field capacity can lead to errors in its simulation. The bucket model cannot reproduce the observed peak of total soil moisture in the top 1 m during the spring snowmelt, since the total soil moisture in the top 1 m of soil rises above the bucket field capacity with the water table in the top meter of soil. As a result, the bucket dries out the soil more quickly in the summer than the observations and then produces lower evaporation rates than the observations during the midsummer, since its soil moisture stores have been depleted. The bucket also produces more runoff than the observations during the fall, since the bucket is at its field capacity, and, as a result, all rainfall is partitioned into runoff. The low degree of interannual variability of the seasonal cycle of total soil moisture during the fall and winter of the bucket, contrary to observations, is also a result of a saturated bucket unable to rise above its field capacity. While the bucket discrepancy may be a site-specific feature, preliminary test results (not reported here) show that a modification to the bucket model that would allow its soil moisture to rise above field capacity and then drain gradually (rather than instantaneously) could produce more realistic soil moisture variations and improve its evaporation and runoff simulations.

While the bucket intercomparison results of this study and RO appear somewhat different from the PILPS results for Cabauw (Chen et al. 1997), these different intercomparison results can be attributed to the bucket model's sensitivity to the value of its drag coefficient and are not a result of differences in the bucket model performance. In the bucket run for Cabauw reported in Chen et al. (1997), the value of the drag coefficient is more than twice as large as the highest value in the typical range for a grassland vegetation (Hartmann 1994). Using a more consistent drag coefficient (calculated using the site-measured roughness length for heat and moisture fluxes), the bucket's anomalous result for the Cabauw simulations was removed (Chen et al. 1997). Our tests with the bucket model using the Russian data of RO (not shown) give sensitivities to the drag coefficient similar to the Cabauw test results.

The most notable discrepancies of SSiB's simulations compared to observations are its lower snow depths and higher summer runoff rates. SSiB's underestimation of snowcover has been attributed to its high amounts of evaporation from the snow surface. We can improve SSiB's snow depth simulation and also reduce the disagreement of SSiB's spring runoff with the bucket and the observations by lowering SSiB's evaporation from the snow surface. A physically consistent modification to correct this feature is currently under investigation (as discussed in the previous section) and will be the subject of a future paper. It should be noted that tests of the Bare Essentials of Surface Transfer (BEST) model (Pitman et al. 1991) with the Russian stations of RO show a similar sensitivity of simulated snow depth to changes in downward longwave radiation (A. Pitman 1996, personal communication). During the summer, SSiB's excess runoff is caused by drainage from the lowest layer rather than surface runoff from the upper soil layer as W_1 is always well below saturation. However, the differences of SSiB's runoff simulations could be due not only to an inconsistent parameterization, but also to inconsistent soil parameters. It seems plausible that SSiB's runoff discrep-

ancies could be corrected by merely varying, within a realistic range of values, its soil parameters not prescribed by observations (Xue et al. 1996a). Moreover, SSiB's evapotranspiration calculations are sensitive to changes in LAI, and LAI was not a measured quantity at Valdai (GCM values for grassland vegetation were used). We can match SSiB's summer rates of evaporation to observations (Fig. 9) by increasing LAI in the summer to values that still fall within a realistic range for a grassland vegetation (Xue et al. 1996b), but it is uncertain whether this is a consistent improvement in SSiB's simulation due to the lack of LAI observations for the catchment. We also did not include any interannual variations of LAI that may occur in nature (e.g., in response to precipitation anomalies) for SSiB's simulations, which is the standard SSiB application for GCMs. As LAI could vary from wet to dry years, some of SSiB's discrepancies seen during the years with extreme hydrologic events may be a result of the lack of an interannually varying LAI. This applies to SSiB's other vegetation parameters as well.

This study has shown, for the first time by diagnosing the complete water budget at seasonal and interannual timescales, that land surface hydrology can be successfully simulated for a midlatitude grassland using only routine meteorological observations as forcing. We continue to build datasets in other climate regimes to test these conclusions with different climates and different vegetation types. Our current efforts include obtaining and utilizing data from additional sites in Russia, Mongolia, China, and India. To date, the Russian data have been used to improve a number of land-surface schemes currently used in GCMs, such as the bucket (Schlosser 1995), SSiB (Xue et al. 1996a), Meteo-France (Douville et al. 1995), BATS (Yang et al. 1997), and SiB2 (Zhang et al. 1996, manuscript submitted to *J. Geophys. Res.*). The Valdai data will be used in the next PILPS effort (Phase 2d) and allow for the first time an international intercomparison study of multiyear land-surface simulations to compare with observations of total soil moisture, runoff, water-table depth, evaporation, and snow depth—the complete water balance. Through continued efforts with data and models such as these, our understanding and parameterizations of land-surface processes can be greatly enhanced. The data used in this study are available to anyone wishing to use them. Please contact the authors.

Acknowledgments. We thank Chris Milly for valuable discussions. This work was supported by NOAA Grants NA36GPO311 and NA56GPO212; and NASA Grants NCC555 and NAGW-5227; and NASA. The views expressed herein are those of the authors and do not necessarily reflect the views of NOAA and NASA.

REFERENCES

Berlyand, M. E., 1956: *Forecasting and Control of the Heat Regime Surface Air Layer.* Gidrometeoizdat, 435 pp.

Berlyand, T. G., 1961: *Distribution of Solar Radiation on Continents* (in Russian). Gidrometeoizdat, 227 pp.

Brutsaert W. H., 1982: *Evaporation into the Atmosphere*. D. Reidel, 299 pp.

Budyko, M. I., 1956: *Heat Balance of the Earth's Surface* (in Russian). Gidrometeoizdat, 255 pp.

Chen, T. H., and Coauthors, 1997: Cabauw experimental results from the Project for Intercomparison of Land-Surface Parameterization Schemes. *J. Climate,* **10,** 1194–1215.

Dickinson, R. E., A. Henderson-Sellers, P. J. Kennedy, and M. F. Wilson, 1986: Biosphere-Atmosphere Transfer Scheme (BATS) for the NCAR Community Climate Model. NCAR Tech. Note NCAR/TN-275+STR, 69 pp. [Available from National Center for Atmospheric Research, P.O. Box 3000, Boulder, CO 80307.]

Domenico, P. A., and F. W. Schwartz, 1990: *Physical and Chemical Hydrogeology*. J. Wiley and Sons, 824 pp.

Douville, H., J.-F. Royer, and J.-F. Mahfouf, 1995: A new snow parameterization for the French community climate model. *Climate Dyn.,* **12,** 21–35.

Fedorov, S. F., 1977: *A Study of the Components of Water Balance in Forest Zone of European Part of the USSR* (in Russian). Gidrometeoizdat, 264 pp.

Golubev, V. S., V. V. Kokneava, and A. U. Simonenko, 1995: Results of atmospheric precipitation measurement with Canadian, Russian, and US standard instruments (in Russian). *Meteor. Hydrol.,* **2,** 102–110.

Hartmann, D. L, 1994: *Global Physical Climatology*. Academic Press, 411 pp.

Henderson-Sellers, A., Z. L. Yang, and R. E. Dickinson, 1993: The Project for Intercomparison of Land-Surface Parameterization Schemes. *Bull. Amer. Meteor. Soc.,* **74,** 1335–1349.

Idso, S. B., 1981: A set of equations for full spectrum and 8–14 μm and 10.5–12.5 μm thermal radiation from cloudless skies. *Water Resour. Res.,* **17,** 295–304.

Manabe, S., 1969: Climate and the ocean circulation, 1. The atmospheric circulation and the hydrology of the earth's surface. *Mon. Wea. Rev.,* **97,** 739–774.

McKenney, M. S., and N. J. Rosenburg, 1993: Sensitivity of some potential evapotranspiration estimation methods to climate change. *Agric. For. Meteor.,* **64,** 81–110.

Milly, P. C. D., 1992, Potential evaporation and soil moisture in general circulation models. *J. Climate,* **5,** 209–226.

——, and P. S. Eagleson, 1982: Parameterization of moisture and heat fluxes across the land surface for use in atmospheric general circulation models. Dept. of Engineering, Massachusetts Institute of Technology Rep. 279, 159 pp. [Available from Massachusetts Institute of Technology, Cambridge, MA 02139.]

Monteith, J. L., 1961: An empirical method for estimating longwave radiation exchanges in the British Isles. *Quart. J. Roy. Meteor. Soc.,* **87,** 171–179.

Pitman, A. J., Z.-L. Yang, J. G. Cogley, and A. Henderson-Sellers, 1991: Description of bare essentials of surface transfer for the Bureau of Meteorology Research Centre AGCM. BMRC Res. Rep. 32, 130 pp. [Available from Bureau of Meteorology Research Center, GPO Box 1289K, Melbourne, Victoria 3001, Australia.]

Rind, D., C. Rosenzweig, and R. Goldberg, 1992: Modelling the hydrological cycle in assessments of climate change. *Nature,* **358,** 119–122.

Robock, A., K. Ya. Vinnikov, C. A. Schlosser, N. A. Speranskaya, and Y. Xue, 1995: Use of midlatitude soil moisture and meteorological observations to validate soil moisture simulations with biosphere and bucket models. *J. Climate,* **8,** 15–35.

Satterlund, D. R., 1979: An improved equation for estimating longwave radiation from the atmosphere. *Water Resour. Res.,* **15,** 1649–1650.

Schlosser, C. A., 1995: Land-surface hydrology: Validation and intercomparison of multi-year off-line simulations using midlatitude data. Ph.D. dissertation, University of Maryland, 135 pp.

[Available from University of Maryland, College Park, MD 20742.]

Sellers, P. J., and J. L. Dorman; 1987: Testing the simple biosphere model (SiB) using point micrometeorological and biophysical data. *J. Climate Appl. Meteor.,* **26,** 622–651.

——, Y. Mintz, Y. C. Sud, and A. Dalcher, 1986: A simple biosphere model (SiB) for use within general circulation models. *J. Atmos. Sci.,* **43,** 505–531.

——, W. J. Shuttleworth, J. L. Dorman, A. Dalcher, and J. M. Roberts, 1989: Calibrating the simple biosphere model for Amazonian tropical forest using field and remote sensing data. Part I: Average calibration with field data. *J. Appl. Meteor.,* **28,** 727–759.

——, D. A. Randall, G. J. Collatz, J. A. Berry, C. B. Field, D. A. Dazlich, C. Zhang, G. D. Collelo, and L. Bounoua, 1996: A revised land surface parameterization (SiB2) for atmospheric GCMs. Part I: Model formulation. *J. Climate,* **9,** 676–705.

Stull, R. B., 1991: *An Introduction to Boundary Layer Meteorology.* Kluwer Academic Publishers, 666 pp.

Sud, Y. C., and M. J. Fennessy, 1982: An observational-data based evapotranspiration function for general circulation models. *Atmos.–Ocean,* **20,** 301–316.

Vinnikov, K. Ya., and M. D. Dvorkina, 1970: Some problems of radiation stations network planning (in Russian). *Meteor. Hydrol.,* **10,** 90–96.

——, and I. B. Yeserkepova, 1991: Soil moisture: Empirical data and model results. *J. Climate,* **4,** 66–79.

——, A. Robock, N. A. Speranskaya, and C. A. Schlosser, 1996: Scales of temporal and spatial variability of midlatitude soil moisture. *J. Geophys. Res.,* **101,** 7163–7174.

Xue, Y., P. J. Sellers, J. L. Kinter, and J. Shukla, 1991: A simplified biosphere model for global climate studies. *J. Climate,* **4,** 345–364.

——, F. J. Zeng, and C. A. Schlosser, 1996a: SSiB and its sensitivity to soil properties—A case study using HAPEX × Mobilhy data. *Global Planet. Change,* **13,** 183–194.

——, H. Bastable, P. Dirmeyer, and P. Sellers, 1996b: Sensitivity of simulated climate to changes in land surface parameterizations—A study using ABRACOS data. *J. Appl. Meteor.,* **35,** 386–400.

Yang, D., 1995: Accuracy of the Tretyakov precipitation gauge: Results of WMO intercomparison. *Hydrol. Processes,* **9,** 877–895.

Yang, Z. L., R. E. Dickinson, A. Henderson-Sellers, and A. J. Pitman, 1995: Preliminary study of spin-up processes in land surface models with the first stage data of Project for Intercomparison of Land Surface Parameterization Schemes phase 1(a). *J. Geophys. Res.,* **100,** 16 533–16 578.

——, ——, A. Robock, and K. Ya. Vinnikov, 1997: On validation of the snow sub-model of the Biosphere–Atmosphere Transfer Scheme with Russian snow cover and meteorological observational data. *J. Climate,* **10,** 353–373.